Unsupervised Deep Video Denoiser: A Potential Key to Extracting Information from Monochromated EELS

Yifan Wang[1*], Carlos Fernandez-Granda[2], Peter A. Crozier[1]

[1.] School for Engineering of Matter, Transport & Energy, Arizona State University, Tempe, AZ, United States.
[2.] Courant Institute of Mathematical Sciences, New York University, New York, NY, USA
[*] Corresponding author: ywan1240@asu.edu

With developments in electron optics, monochromated electron energy-loss spectroscopy (EELS) coupled with scanning transmission electron microscopy (STEM) makes characterizing materials properties, e.g., phonon [1], with both high energy (~10meV) and spatial (<1Å) resolution feasible. One of the disadvantages of this method is the low signal, especially for some special techniques, e.g., off-axis EELS [2]. The most common way to compensate for the low signal is to acquire the data with longer exposure time. However, this can amplify some problems: instability of the electron optics, radiation damage, sample drifting, etc. Is there a way to further reduce the time for acquiring the data while still being able to extract the same information? The development of the detector technology, i.e., the direct electron detectors, has limited the readout noise thus making high-quality high-speed (or low-dose) readout possible [3]. With the help of convolutional neural network, an unsupervised deep video denoiser (UDVD) has been applied successfully in denoising low-dose TEM images [4]. In this work, we are demonstrating that the UDVD can also be applied to EELS with low signal acquired using direct electron detectors.

Here we show the UDVD combined with a new workflow (**figure 1a**) to extract information from low signal energy-loss dataset. Series of energy-loss spectra are acquired and recorded as images (without integrating in the non-dispersive axis), so that all the information in the data is preserved. The dataset is uploaded to the supercomputer (ASU Sol [5]) and processed with the UDVD. After denoising, post-processing can be applied to extract information from the dataset, including zero-loss peak alignment, generation of spectrum images, etc. **Figure 1b** shows the results from the denoising and the raw data, which is constructed by 2500 spectra. By summing and comparing multiple frames in the raw and denoised data, we can identify artifacts and gain information about the quality and accuracy of the output. As the number of the frames (total signal), increases, the denoised result resembles the raw data. This indicates the denoiser is generating reasonable results. We have also calculated a nominal signal-to-noise ratio (SNR) of a relatively uniform part in the image. For a single frame, the 'SNR' increased by at least a factor of ~10 after denoising, and the raw data has reached a similar 'SNR' after summing 1000 frames.

We applied the UDVD on an off-axis vibrational EELS mapping of hexagonal boron nitride (h-BN). Preliminary was acquired on a Nion UltraSTEM 100 equipped with a Dectris ELA hybrid-pixel detector [6] as the camera for the energy-loss spectrometer. We used a 33 mrad probe with a beam current of 250 pA, and the size of the probe is ~ 90 pm. The h-BN sample was tilted into [0001] zone axis and a high-angle annular dark-field (HAADF) image was acquired (**figure 2a**). To perform the off-axis EELS, the (000) beam of the diffraction pattern was shifted 66 mrad away from the 1mm EELS entrance aperture so that the (000) beam is excluded [7]. The energy resolution was measured to be 18 meV (ZLP full width at half maximum), and the beam current entering the spectrometer is $4.5*10^{-3}$ pA. We performed the EELS mapping on an 8x8Å area (indicated as the red box in **figure 2a**). The map is constructed by 50x50 spectra with 100ms exposure time. The result reading from the HAADF detector is shown as **figure 2b**, denoted as 'BF' (since most of the BF disk was shifted on to the HAADF detector). The whole dataset was denoised with the UDVD and the image of the spectrum was integrated along the non-dispersive direction. **Figure 2c** shows the sum of the whole spectrum image for the raw data and the denoised data. The two spectra show perfectly match, and three peaks can be observed corresponding to TA, LA, and TO-LO phonon branches of h-BN. To demonstrate the capability of the UDVD, a series of spectrum image is presented here (**figure 2d**). After denoising, the ZLP spectrum image and the total inelastic signal have less noise. As we select a smaller energy window (10 meV in our case) for specific phonon peaks, the denoised spectrum image still resemble the structure, especially the TA peak, while the raw data are dominated by noise. **Figure 2e** shows a single spectrum on the atomic column (orange box) and off the atomic column (blue box). The intensity dropped when the beam is moved from the atomic column to the hole, especially the TA phonon (indicated by the red arrow). The shape change of the spectrum shows that the denoiser can differentiate the miniscule difference between spectra. Application of the UDVD and the workflow to other scenes, e.g., other vibrational EELS measurement including E-q curve measurement, valence-loss EELS, core-loss EELS, etc., will also be presented.

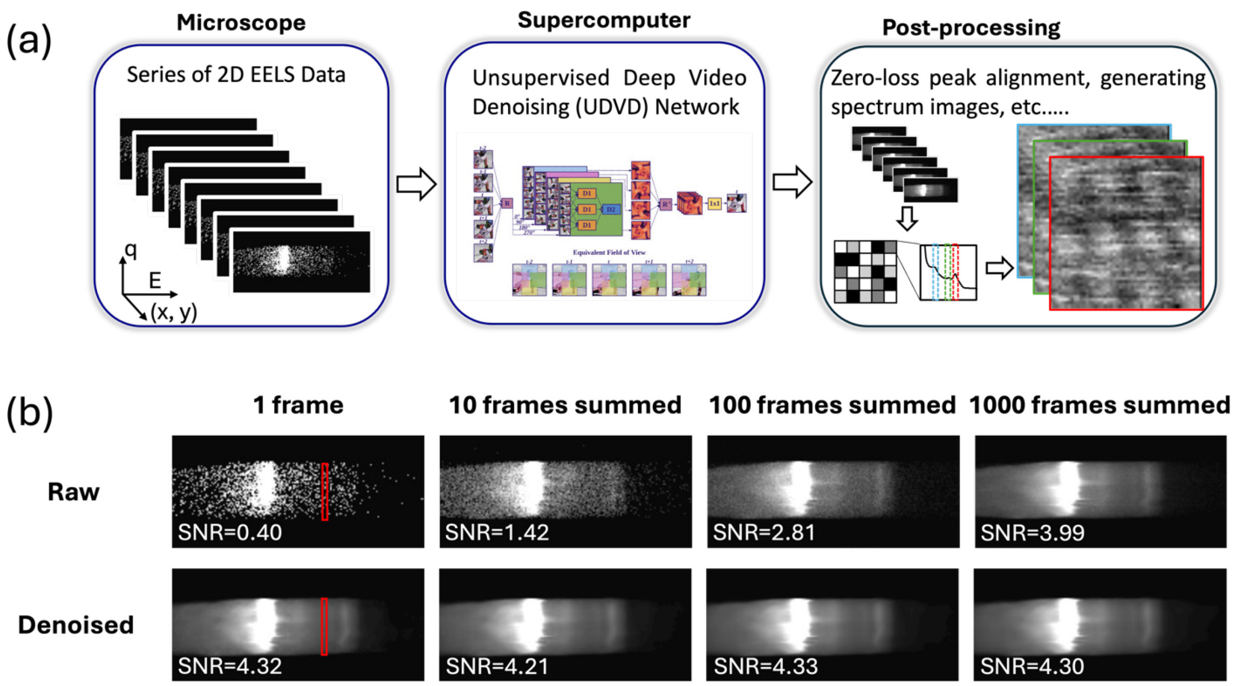

Figure 1. (a) The workflow designed for denoising low-dose EELS series. The axes of the dataset are energy-loss (E), non-dispersive direction (q), and spatial coordinates ((x,y)). **(b)** The comparison between raw data and denoised results. The brightness and contrast are set to the same for all the images. A relatively uniform part of the spectra (red box) is selected to calculate SNR, defined as mean divided by standard deviation (This is not the SNR for the whole image.) The 'SNR' of each image is calculated.

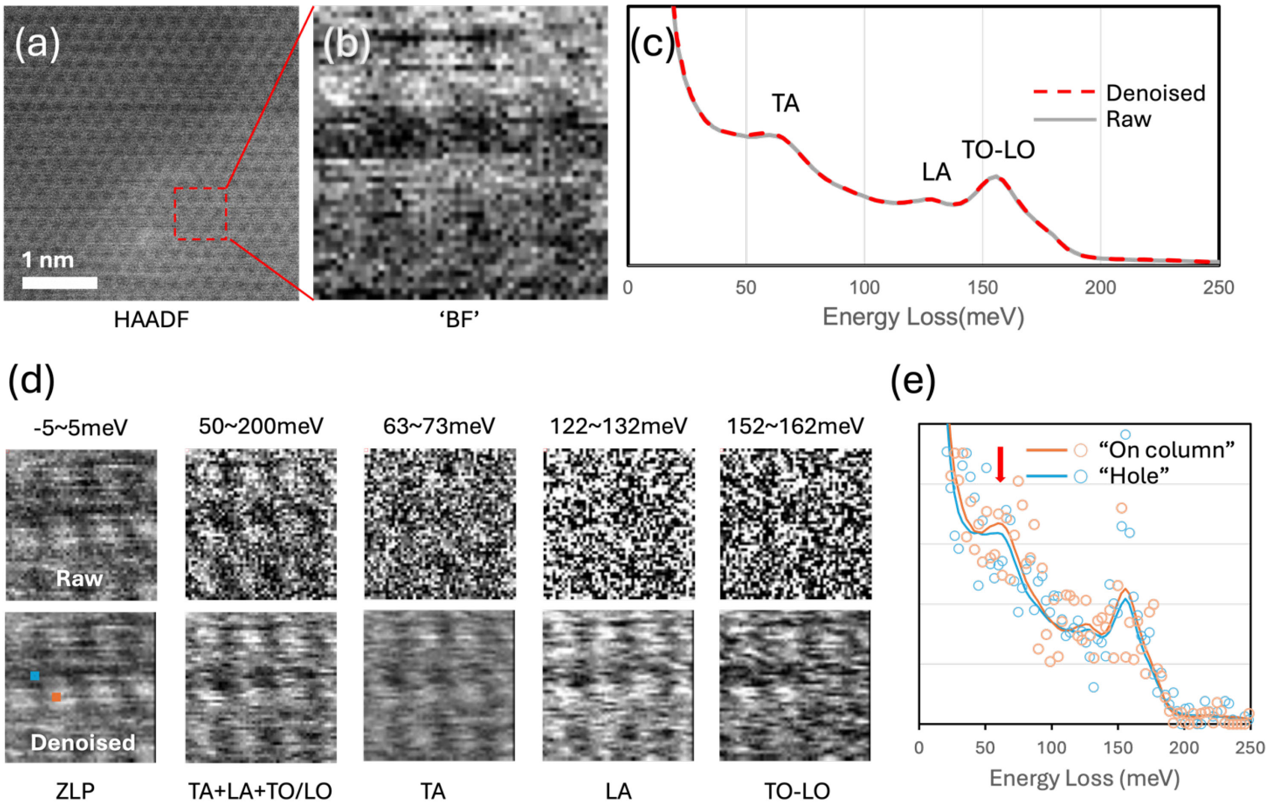

Figure 2. Results from an off-axis vibrational EELS map of h-BN. **(a)** The HAADF image of the sample. The red box shows the area where the spectral mapping was taken. **(b)** The signal collected from HAADF detector in the off-axis mapping, denoted as 'BF'. **(c)** The summed energy-loss spectra from the whole spectral mapping. The gray curve is the raw data and the red dashed curve is the denoised data. Three features are visible at around 63~73 meV, 122-132 meV, and 152~162 meV, corresponding to h-BN's TA, LA, TO-LO phonons, respectively. **(d)** Spectrum images generated from the raw data and denoised data. The top row is the raw data, and the bottom row is the denoised data. Energy range that used to generate spectra images are above the figures and their corresponding features are at the bottom. The brightness and contrast are set to the same for each set of the raw and denoised dataset. **(e)** Single spectrum from different areas. The orange spectrum is collected on the atomic column while the blue spectrum is collected off the atomic column ('hole'), shown in the ZLP spectrum image (**figure 2d**). The line and circle represent denoised and raw data, respectively. The change in the TA peak is denoted with a red arrow.

References:

[1] F. S. Hage *et al.*, Science **367**, 1124 (2020).
[2] C. Dwyer *et al.*, Phys. Rev. Lett. **117**, 1 (2016).
[3] A.-C. Milazzo *et al.*, J. Struct. Biol. **176**, 404 (2011).
[4] D. Y. Sheth *et al.*, in *Proc. IEEECVF Int. Conf. Comput. Vis.* (2021), pp. 1759–1768.
[5] D. M. Jennewein *et al.*, in *Pract. Exp. Adv. Res. Comput.* (Association for Computing Machinery, New York, NY, USA, 2023), pp. 296–301.
[6] B. Plotkin-Swing *et al.*, Ultramicroscopy **217**, 113067 (2020).
[7] F. S. Hage *et al.*, Phys. Rev. Lett. **122**, 16103 (2019).

[8] We gratefully acknowledge support of NSF grants to ASU (CHE-2109202, OAC 1940263, 2104105) and NYU (HDR-1940097 and OAC-2103936). We also gratefully acknowledge the use of ASU's John M. Cowley Center for High Resolution Electron Microscopy and the Sol supercomputer at ASU.